Aerodynamic and Aeroacoustic Wind Tunnel Testing of the Orion Spacecraft

James C. Ross[1]
NASA Ames Research Center, Moffett Field, CA 94035 USA

The Orion aerodynamic testing team has completed more than 40 tests as part of developing the aerodynamic and loads databases for the vehicle. These databases are key to achieving good mechanical design for the vehicle and to ensure controllable flight during all potential atmospheric phases of a mission, including launch aborts. A wide variety of wind tunnels have been used by the team to document not only the aerodynamics but the aeroacoustic environment that the Orion might experience both during nominal ascents and launch aborts. During potential abort scenarios the effects of the various rocket motor plumes on the vehicle must be accurately understood. The Abort Motor (AM) is a high-thrust, short duration motor that rapidly separates Orion from its launch vehicle. The Attitude Control Motor (ACM), located in the nose of the Orion Launch Abort Vehicle, is used for control during a potential abort. The 8 plumes from the ACM interact in a non-linear manner with the four AM plumes which required a carefully controlled test to define the interactions and their effect on the control authority provided by the ACM. Techniques for measuring dynamic stability and for simulating rocket plume aerodynamics and acoustics were improved or developed in the course of building the aerodynamic and loads databases for Orion.

I. Introduction

The Orion spacecraft will provide human access to space from low earth orbit to potential missions to asteroids and beyond. In order to successfully carry out its various missions, its flight behavior in Earth's atmosphere must be accurately understood and controlled. The aerodynamic database for the Orion is being developed by a combination of wind tunnel tests and Computational Fluid Dynamics simulations and will allow accurate flight simulations to verify the performance, controllability, and safety of the vehicle during all phases of atmospheric flight.

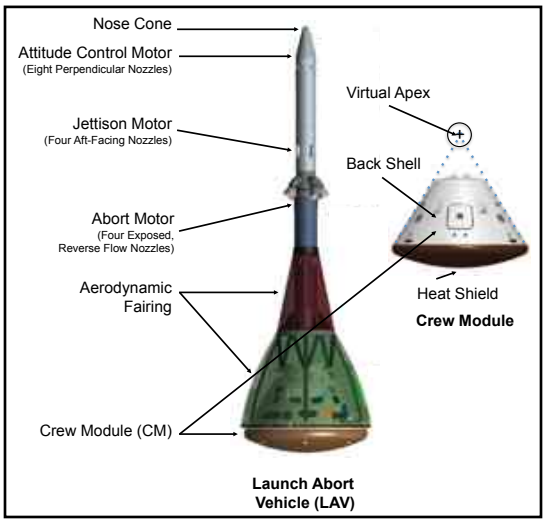

Figure 1. Components of the Orion space-craft.

Figure 1 shows the Orion and its components. The Crew Module (CM) is the heart of the vehicle and carries the crew throughout the flight. During launch and ascent through the atmosphere, the aerodynamic fairing protects the CM and crew from the high levels of aeroacoustic noise resulting from the high dynamic pressure experienced during ascent. The Launch Abort Tower (LAT) is made up of the aerodynamic fairing and the tower containing the various rocket motors needed accomplish a launch abort (Abort Motor and Attitude Control Motor). It also carries the Jettison Motor that is used to separate the LAT from the CM after a successful launch or at the appropriate point during a launch abort to allow deployment of the CM parachutes.

For re-entry and descent, defining the CM aerodynamics, both static and dynamic, is important in order to ensure stable and controllable flight from re-entry and hypersonic flight down to the subsonic parachute deployment. During

[1] Aerospace Engineer, Experimental Aerophysics Branch, MS 260-1, Associate Fellow AIAA.

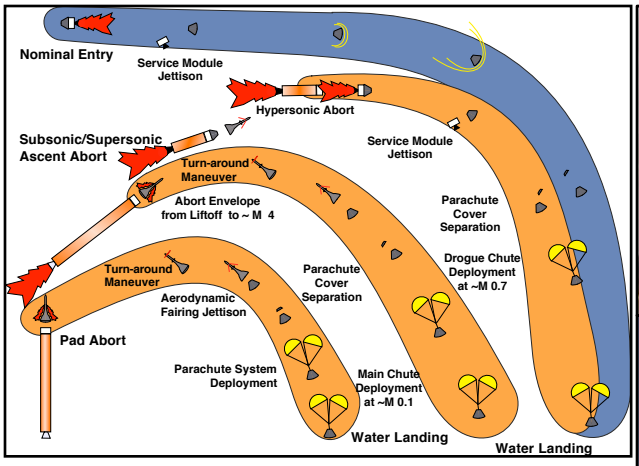

Figure 2. Phases of Orion flight during which aerodynamics and aeroacoustics are important.

Figure 3. Phases of Orion launch abort flight taken from PA-1 videos (Pad Abort test). From upper left: pre-ignition, boost phase, coast phase, turn around maneuver, tower jettison, and parachute deployment. Note that the PA-1 vehicle was an older configuration with a different aerodynamic fairing shape.

the ascent from the launch pad to orbit, ensuring successful launch aborts at altitudes below 100,000 feet (and Mach number less than 4.5) is a critical concern for the vehicle designers. Since a launch abort would use both the high-thrust Abort Motor (AM) to provide rapid separation from the launch vehicle and the much lower thrust Attitude Control Motor (ACM) for steering the LAV, accurate assessment of the aerodynamic effects of both sets of rocket plumes is essential.

The phases of launch and recovery that must be accurately modeled in the aerodynamics database are shown in Figure 2. During a nominal ascent, the Aerodynamic Fairing protects the CM and crew from large fluctuating pressures on the surface. The fairing also protects the CM from both the high noise levels and heat in the event of a launch abort when plumes from the high-thrust AM pass close to the surface of the LAV. Figure 3 depicts the phases of flight during a pad abort flight test. These flight phases would also be experienced during an abort from other points in the launch trajectory. During the boost phase of an abort, it is critical to know the aerodynamic behavior of the LAV accurately as it pulls away from the launch vehicle (includes booster, second stage, and the Orion Encapsulated Service Module or ESM) so that satisfactory control of the vehicle can be assured given the capabilities of the ACM. In fact, one of the critical measurements was to determine the installed performance of the ACM over a wide range of flight conditions. Because the ACM plumes interact with the Orion vehicle (which is downstream of the ACM for most of any LAV flight), the effect of this plume interaction can, in certain situations, result in a significant reduction in the control efficiency of the ACM system. Determining this interaction, particularly during the boost phase of abort flight, took considerable effort. In particular, the boost-phase of an abort, the ACM plumes interact very nonlinearly with the AM plumes resulting in a very complicated aerodynamic database.

There have been more than 40 individual tests of the aerodynamics and aeroacoustics of the Orion so far. Most of the tests were conducted in wind tunnels but a few were run in ballistic ranges and other types of laboratories. Approximately 10% of the testing hours were used to address the static aerodynamics of the CM at M 4.5 and below. An additional 20% were to define the dynamic stability of the CM for Mach numbers from 0.1 to about 2. Most of the remaining test hours have been spent

documenting the aerodynamics and acoustics of the LAV for a large variety of potential flight conditions that might occur during launch aborts within the atmosphere. The powered testing required to simulate this portion of the possible flight of the Orion has been the most challenging to perform and the various test teams have accomplished the tests successfully using combinations of innovative test techniques and clever model designs. A list of the Orion wind tunnel tests conducted to date is given in Table 1 in Appendix A.

II. Aerodynamic Testing

In 2007 the aerodynamic testing completed up to that point and the plan for subsequent testing was presented.[1] Since then, a majority of the planned testing has been completed along with several tests that were added to address particular flight conditions and design changes. So far, tests have been conducted in 19 different wind tunnels, 4 ballistic ranges, and 3 research laboratories across the US. The tests have covered a Mach number range of 0.05 to ~20. A few tests have yet to be completed which will address additional questions about wind-tunnel-to-flight extrapolation and the effects of changes to the vehicle design and ascent trajectory that will result from using a rocket other than the canceled Ares-1 to launch Orion.

A. CM Static Aerodynamics

The first testing done for Orion was to define the static aerodynamics of the Crew Module. For the most part, the data does not need updating except to document the effect of a change in the back shell angle since the early tests and the effect of going from wind tunnel conditions to flight conditions (effect of Reynolds number, primarily). Six tests documenting the CM static aerodynamics have been run with the remaining CM test planned for the National Transonic Facility. Figure 4 shows the models used in three of the CM tests that covered the Mach number range of 0.3 to 6. These tests were done in the Unitary Plan Wind Tunnels located at NASA's Ames and Langley Research Centers and in the Langley 20-Inch Mach 6 Air Tunnel. These tests have been reported on previously.[2 - 5]

The fourth model in the figure is a CAD rendering of a model being built for testing in the National Transonic Facility at NASA's Langley Research Center. That test will provide the data at or near flight Reynolds numbers up to Mach 0.9 which will help to extrapolate the aerodynamic database to flight conditions. Of particular interest is using the low- to high-Re aerodynamic increments to verify similar increments generated using CFD since the computational tools are the principle means to provide increments from wind-tunnel to flight conditions.[6,7] The hypersonic portion of the aerodynamic database for the CM has been generated primarily using CFD[8] with anchoring data provided from a test at the Mach 6 Air Tunnel at NASA Langley.

While much of the static aerodynamics testing standard wind-tunnel techniques and instrumentation, the use of Pressure Sensitive Paint (PSP) was very helpful in providing a more detailed understanding of the flow around the models.[9,10] The changes in the aerodynamics are much more easily interpreted when a detailed pressure distribution is measured over the entire body. During tests of the CM there were

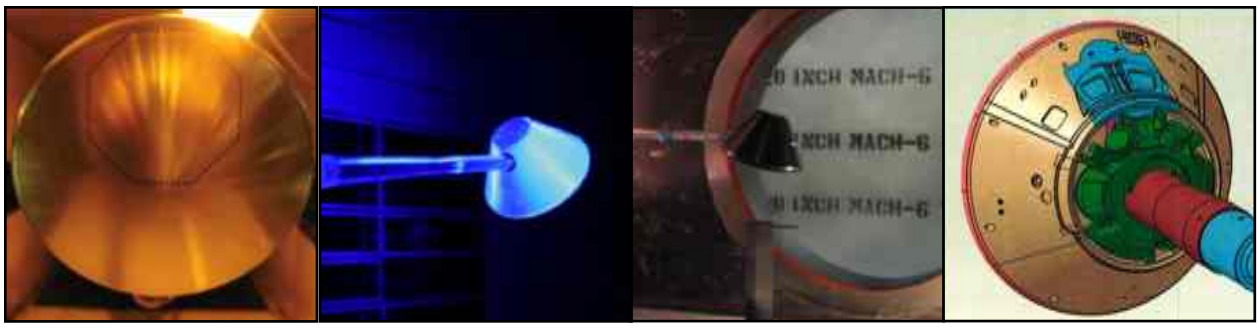

Figure 4. CM static aero testing. From left to right: 3%-scale model in NASA Langley Unitary Plan Wind Tunnel, 7.5%-scale model in NASA Ames Unitary Plan Wind Tunnel, 2%-scale model in the NASA Langley 20-Inch Mach 6 Air Tunnel, and a rendering of a 5%-scale model design for high-Reynolds Number testing in the NASA Langley National Transonic Facility.

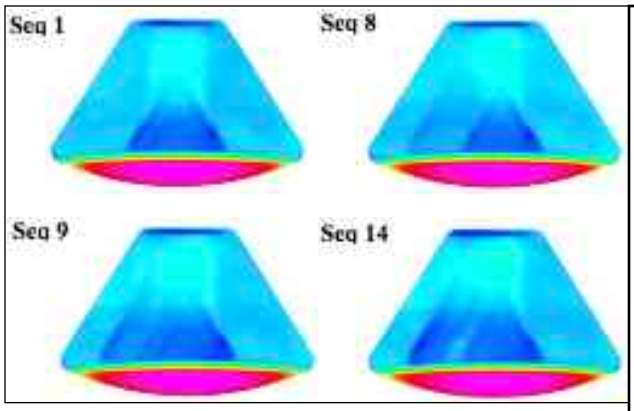

Figure 5. Changing pressure distribution over CM at M 0.95, α = 142°. The heat-shield boundary layer is not tripped. Each image represents a relatively long exposure time of ~2 seconds.

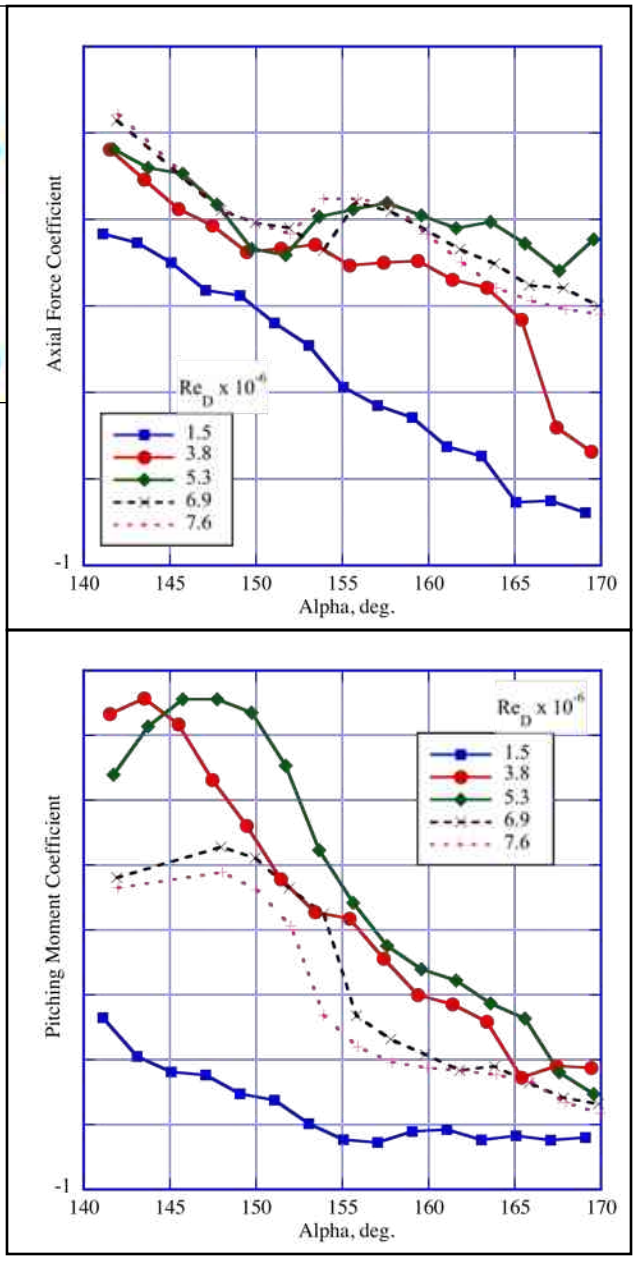

Figure 6. Effect of Reynolds number on CM aerodynamics at M 0.5. Axial force coefficient (top) and pitching moment coefficient (bottom).

some conditions that had large scatter in the forces and moments. It was evident from the force data that large unsteadiness in the aerodynamics caused the increase in uncertainty. Examination of the PSP data showed quite clearly that for these particular conditions, there was an unstable separation pattern driving the unsteady aerodynamic forces and moments. For example at Mach 0.95 and angles of attack from 140 to 155° (180° is heat shield directly into the wind), none of the aerodynamic coefficients repeated well from run to run. Figure 5 shows PSP images at four different sequence numbers that show different separation patterns occurring at the same test condition (Mach 0.95 and 142° angle of attack). Consecutive sequence numbers were acquired 7.5 seconds apart and each represents a 2 second exposure. Sequence 1 shows the flow pattern that was seen the most often. Sequence 8 shows evidence of a second flow pattern shifted to the right that occurs for a considerably shorter time since the dominant pattern is much more pronounced. Sequences 9 and 14 indicate nearly equal likelihood for the two flow patterns with a third pattern in between. These data were acquired at a Reynolds number of 6.9×10^6 with no boundary layer trips on the heat shield. Tripping the boundary layer on the heat shield has a significant effect on the aerodynamics, particularly the axial force coefficient, but did not change the flow unsteadiness at this particular test condition.

An important parameter examined for all static aerodynamics tests is Reynolds number. In most of the wind tunnels used for Orion testing, the maximum Re for a given Mach number was 20% or less of the value expected for flight. This means there is a significant extrapolation required and the Re trends are not simple to interpret and definitely not monotonic with Re. Figure 6 shows the trends for axial force and pitching moment coefficients with Re for a Mach 0.5 free stream. In both figures 6a and 6b, it is clear that the Re effect depends on the angle of attack and is different for axial force and pitching moment. Most of the data acquired for the CM (and other configurations) was with trips applied. We

Figure 7. Aerodynamic fairing designs tested.

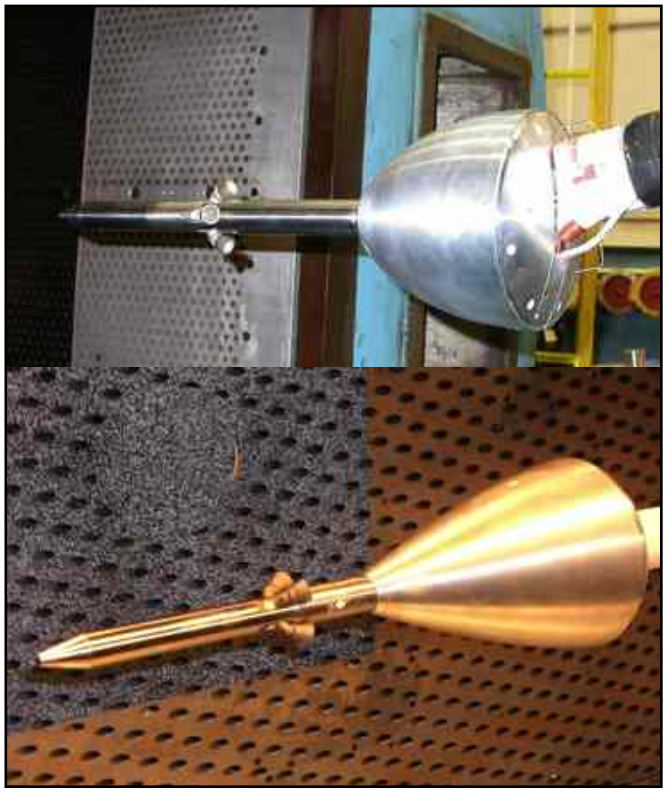

Figure 8. Wind-tunnel models of ALAS-11 in the Boeing Polysonic Wind Tunnel (top) and ALAS-11 rev 8 in the AEDC 4T wind tunnel (bottom).

have primarily used mylar dots estimated to be tall enough to trip the flow and on the heat shield, the pattern is shown in the left-hand photo in Figure 4. The intent is to always have the stagnation point inside the ring at all angles of attack and sideslip so the flow has to cross a trip as it heads radially outward. The rules of thumb are not well established for heat-shield tripping and remains a point of study for the aerodynamic testing team.

The subsonic flight Re data will be determined during a planned test at the NASA Langley National Transonic Facility. This test will also provide updated aerodynamics for the changes to the CM configuration including geometric details and a change in the back-shell angle since the earlier CM aerodynamic testing.

B. LAV Static Aerodynamics

Several tests of the unpowered Launch Abort Vehicle configuration have also been completed. Initially these tests were used to define the coast-phase aerodynamics - after the AM burnout and without the ACM firing. While not an actual flight condition, the intent was to build the database incrementally from unpowered aerodynamics with increments for the effects of the AM and ACM firing. During these tests, several alternative shapes for the aerodynamic fairing were tested. Estimates of fluctuating pressure levels while passing through the atmosphere were unacceptably high for the original 605 shape so a redesign was undertaken. Figure 7 shows several of the alternative designs. Shapes were developed using CFD with the goal of eliminating separation bubbles, primarily those at the forward facing conical intersections, and the rapid expansion and separation at the sharp corner transition to the ESM on the 605 configuration. The NASA Engineering and Safety Center took on the redesign effort (principally Steven Bauer at NASA Langley Research Center) and developed a family of tangent-ogive shapes referred to as ALAS (Alternate Launch Abort System). All of the new shapes had the desired effect of reducing the

fluctuating pressure load on the LAV but also reduced it's static stability. The ALAS 11 shape was eventually adopted as a reasonable compromise between reduced aeroacoustic loads and decreased stability. During testing at the Boeing Polysonic Wind Tunnel, the aeroacoustic levels were still excessive at the junction between the tower and the ogive shape so fairings were tested (referred to as the rev 2 and rev 3 configurations). Both successfully reduced the levels with minor increases to the instability and the rev 3 configuration was adopted. Work continued on alternative shapes resulting the ALAS 11 rev 8 and rev 10 configurations. These had good aeroacoustic and aerodynamic characteristics but by the time testing in the AEDC 4T wind tunnel confirmed the performance, the cost of another change to the LAV shape led to retaining the rev 3 shape. Figure 8 shows the testing at the Boeing Polysonic Wind Tunnel and the AEDC 4T Wind Tunnel.

A high-Reynolds number test of the LAV was also performed in the National Transonic Facility at NASA Langley.[11] This test provided important data concerning the effect of Re on the coast-phase, unpowered aerodynamics of the LAV and the efficacy of the trip dot patterns that have been standardized across all of the LAV tests.

C. CM and LAV Dynamic Stability

During re-entry, the CM is both statically and dynamically stable at hypersonic and supersonic conditions. As it slows to subsonic speeds it remains statically stable (at the design center of gravity) but the dynamic stability decreases and at some angles of attack the CM is dynamically unstable. Because of it's importance to crew safety and the wide variety of conditions it may have to fly through, determining the dynamic stability of the LAV was also a high priority. So far, 13 tests of the CM dynamic stability have been conducted with another 5 to document dynamic stability of the LAV. The testing was done in a variety of wind tunnels and ballistic ranges. Wind tunnel testing included small- and large-amplitude forced oscillation as well as free-flight tests at several ballistic ranges and in the Vertical Spin Tunnel at NASA's Langley Research Center. Figure 9 shows dynamically-scaled CM models flying in a ballistic range at supersonic conditions and in the Vertical Spin Tunnel.

The majority of the dynamic stability data used in the aerodynamic database for the CM alone was obtained from forced-oscillation testing in the Transonic Dynamics Tunnel (TDT) at NASA Langley Research Center. Figure 10 shows two of these tests with the models mounted to a transverse shaft spanning the 16-foot test section. A hydraulic motor is used to drive the shaft for the forced oscillation testing while the aerodynamic data is obtained from an internal balance in the model. These models need not be dynamically scaled but the shaft must pass through the center of gravity expected for the flight

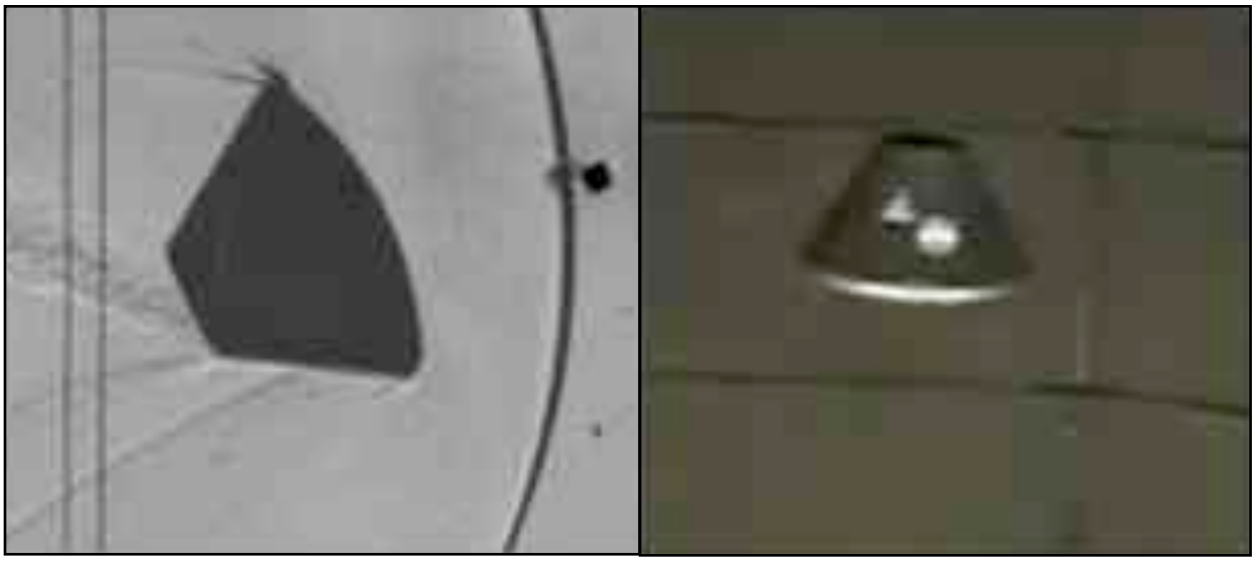

Figure 9. Dynamic stability testing of the Orion Crew Module. Supersonic test in Ames High-Speed Free-Flight Aerodynamics Facility (left) and low-speed test in the Langley Vertical Spin Tunnel (right).

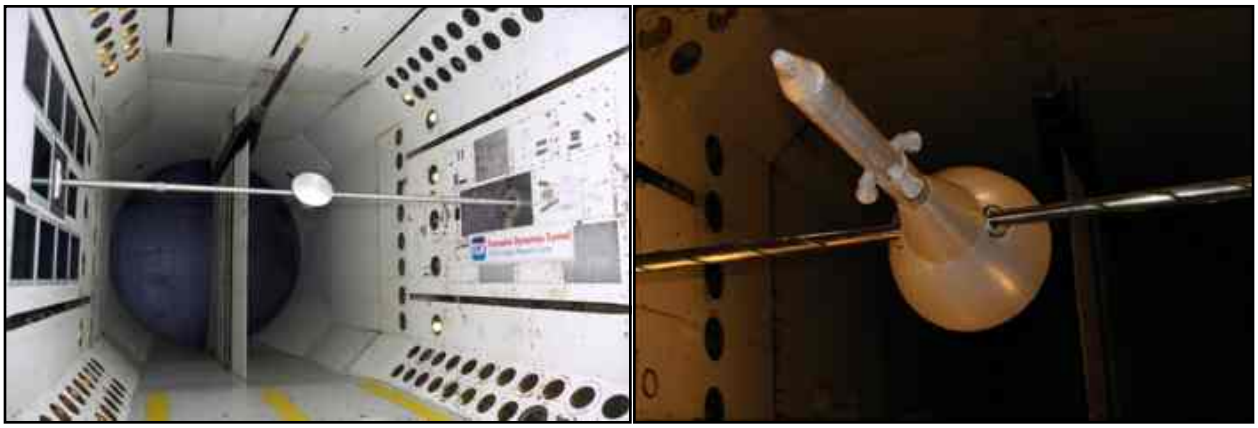

Figure 10. Large amplitude forced oscillation testing in the NASA Langley Transonic Dynamics Tunnel. Crew Module (left) and Launch Abort Vehicle (right).

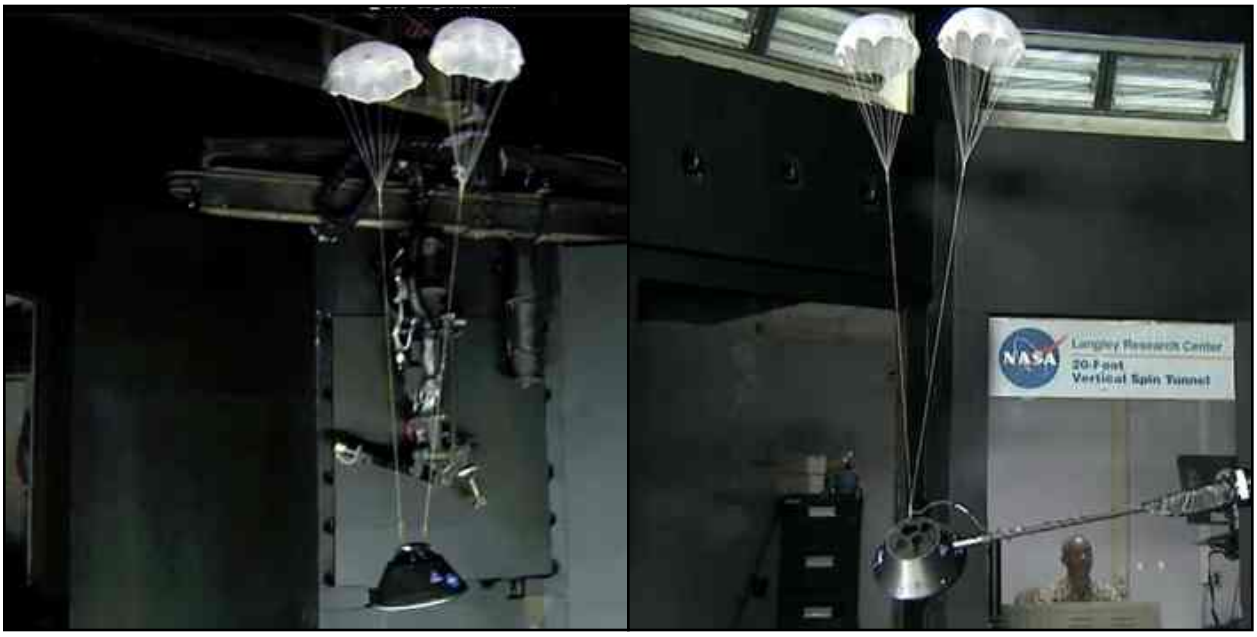

Figure 11. Dynamic stability testing of the Orion Crew Module with drogue parachutes in free flight (left) and on forced-oscillation test rig (right).

vehicle. Inertial tares are obtained to remove the effect of the model mass allowing the aerodynamics forced due to the model motion to be determined. The TDT can run with heavy gas and at elevated pressure to achieve relatively high Reynolds numbers which was important to ensure there are no dramatic changes in dynamic stability at high Re. The engineers who worked on aerodynamics for Apollo relied on free-to-oscillate testing using mounting systems that look very similar the the TDT system. A feature of the TDT system was the ability to also test with the model free to oscillate. The dynamic stability for the Orion CM was found to be similar to that of Apollo, perhaps not surprising given the physical similarities between the two vehicles. The dynamic stability testing for Orion is described in more detail in references 13-16.

The dynamic stability of the CM under the drogue parachutes is another potential problem that had to be addressed. A series of tests were performed in the Vertical Spin Tunnel to determine whether there were significant changes to the dynamic stability when the parachutes were deployed. Two of these tests are shown in Figure 11. The photo on the left shows the CM and drogue chutes in free flight in the wind tunnel while the photo on the right shows the combined model mounted on a forced oscillation rig. In the

forced oscillation test the drogue chute loads were measured using a load cell in the riser while the balance in the CM model measured the overall load. This arrangement allowed us to separate the CM and parachute forces and moments providing detailed understanding of the CM dynamic stability under the drogue chutes.

D. Powered Testing for Launch Abort Vehicle Aerodynamics

By far, the largest effort in aerodynamic testing has been spent defining the performance and controllability of the LAV including the effects of the AM and ACM plumes. Several tests were performed to separately define the jet interactions of the plumes from the two motor systems. Unfortunately the two sets of plumes also interact with each other in very nonlinear ways so another test was performed in order to include the combined effects for as many conditions as possible. The jet interactions are important for the LAV since it has to fly safely from Mach 0 through ~4.5 with significant atmospheric effects and the reliability of the abort system must be better than 95% for all flight conditions. CFD analyses and subsequent wind-tunnel testing showed that the aerodynamic interactions with the AM plumes, for example, could significantly degrade the control authority available to maintain the desired flight trajectory. CFD also showed that the two sets of plumes interact, often unfavorably, in very non-linear ways, further complicating the development of an accurate aerodynamic database for the powered phase of potential launch aborts.

A third rocket motor, the Jettison Motor (JM) is used to separate the Launch Abort Tower from the Crew Module. This motor has 4 flush nozzles located on the upper tower forward of the AM nozzles. It's purpose is to separate the LAT from the CM either during a nominal launch (after the possibility of the LAT being needed for an abort) or after the turnaround maneuver during a launch abort. Testing was performed to simulate the jettison event during an abort to determine the jet interactions because of possible upsetting moments on the CM.

Powered testing to determine the interactions between the rocket plumes and the vehicle has an inherent limitation due to the specific fluid properties of the hot rocket plumes on the real vehicle relative to the properties of the gas used to simulate the plumes in a wind tunnel. Most wind tunnels do not allow tests with live rocket motors but even for tunnels that do, the test durations that can be generated from a test with a solid rocket motor are so short that only a single test condition can be examined for every rocket firing. Building a database using this kind of test procedure would be prohibitively expensive so we took a different approach.

There is a great deal of information in the literature concerning plume matching for a variety of vehicles and plume types. The engineers on the Apollo Project used their experience with hydrogen peroxide for simulating jet-engine plumes[17] to perform powered tests of the Launch Escape System simulating the plumes by decomposing hydrogen peroxide in a catalyst bed located in the Launch Abort Tower of a wind-tunnel model.[18] In the intervening years the engineers having experience with hydrogen peroxide plume simulation have mostly retired and the systems used for the simulations have long disappeared. For Orion, we chose to use high-pressure air (HPA) for the simulations in the wind tunnel and to correct the wind-tunnel data to flight conditions and exhaust gases using CFD. This eliminated the need to develop an expensive, and probably limited use, plume-simulation system but it meant we had to rely on CFD to properly correct the wind-tunnel data to represent what would happen with flight-like plumes.[19,20] The AM and ACM rocket motors on the LAV have exhaust temperatures measured in thousands of degrees F and very high chamber pressures. The HPA available at most wind tunnels is limited to a few hundred degrees but can be delivered to a model at very high pressures and mass flows. The mismatch in the temperature leads to a large difference in the speed of sound in the plume while the difference in chemical constituents leads to a mismatch in γ. As a result, the plume velocity in the simulated plumes do not match flight values causing the flow entrainment to be incorrect relative to flight and the plume shape is different than flight unless care is taken in how the plumes are simulated.

In order to do the best plume matching possible, a study of the important parameters and their various effects on the plume trajectory and shape was done.[21] The principle parameter that was matched was the thrust ratio defined as:

$$Thrust\ ratio = T / (q_\infty S)$$

Figure 12. 6%-scale Jettison Motor jet interaction test model in the 14x22-Foot Wind Tunnel at NASA Langley Research Center (left) and 7%-scale model in the AEDC 16T wind tunnel (right).

where T is the motor thrust, q_∞ is the free-stream dynamic pressure, and S is the vehicle reference area. This parameter allows a first order match of the penetrating power of the plumes against the force of free-stream dynamic pressure turning the plumes toward the free-stream direction. By simultaneously matching the exit Mach number (M_e) of the plume gases by designing the necessary nozzle area ratio, two parameters are matched. A further correction to this scaling includes the effect of γ differences by using one of the following matching parameters instead of exit Mach number alone:

$$\gamma M_e^2 \text{ or } \gamma M_e^2 / (1 - M_\infty^2)^{\frac{1}{2}}$$

depending on the point in the trajectory (Mach number and altitude) being simulated.

1. Jettison Motor Jet Interaction Testing

After the turnaround maneuver during a launch abort the LAT (tower and aerodynamic fairing in Figure 1) is jettisoned (Figures 2 and 3). Ensuring that this event is safe, i.e. no recontact between the LAT and the Crew Module, is important to ensure the success of any potential aborts. A series of tests were performed to simulate the jettison event for Mach numbers from around 0.1 up to 2.5.[22] The low-speed testing was done in the 14-by 22-Foot Wind Tunnel at NASA Langley Research Center. The transonic testing was done in the 16T Wind Tunnel at AEDC while the supersonic tests were done in the 9x7 at NASA Ames Research Center. Figure 12 shows the models mounted in the 14x22 and 16T. The models could be arranged to simulate a variety of axial and vertical separations and angular displacements of the LAT relative to the CM. The models have balances in both the CM and the LAT so that the mutual aerodynamic interference is measured. The tests also looked at both parts of the vehicle in isolation. Running with and without the JM simulation provides the necessary data to compute the jet interactions for all of the relative positions of the CM and LAT.

Figure 13. Abort Motor plume CFD validation test in the HFJER at NASA Glenn Research Center.[23]

2. Abort Motor Jet Interaction Testing

Early in the process of developing the aerodynamic database we recognized that assuming linearity between the jet interaction of the AM and ACM plumes was not correct. Unfortunately, the

difficulty of doing a combined AM and ACM test was such that there was no choice but to make that assumption at least for the early versions of the database. Two tests were run looking at just the AM jet interactions but with relatively crude plume matching. The plan was to use these test results as a start on the database and to verify the accuracy of the available CFD tools. The bulk of the aerodynamic database was then going to be generated using CFD. The CFD results were not as reliable as hoped so a simpler validation experiment was run to help identify the shortcomings and perhaps some fixes to the computational tools.

The problem was simplified to a single nozzle that could emit either cold or hot high-pressure air. One of the major differences between the high-pressure air plume simulations and the solid rocket motor plumes is the exit temperature (~300K versus several thousand K). The validation experiment was able to run cold air (~300K) or heated air (up to ~800K) using the High Flow Jet Exit Rig (HFJER) at NASA's Glenn Research Center.[23] The experimental set up is shown in Figure 13. For this test the LAV shape was simplified by eliminating the tower between the nozzle and the rest of the LAV model. The single nozzle fed by the HFJER was mounted above the normal plenum for the facility. A co-flowing wind tunnel surrounds the HFJER and can run at up to M 0.3. Three-component Particle Image Velocimetry measurements were made in planes parallel and perpendicular to the free stream. The nozzle angle relative to the free stream could be set to 0°, 25° or 40° and the LAV model could be removed or set at a variety of positions and angles relative to the nozzle. Figure 14 shows measured velocity distributions in a plane bisecting the plumes from the 25° and 40° offset nozzles. Shestopalov[24] presents a summary of the CFD efforts to improve the prediction capabilities for hot plumes based on the data from this test.

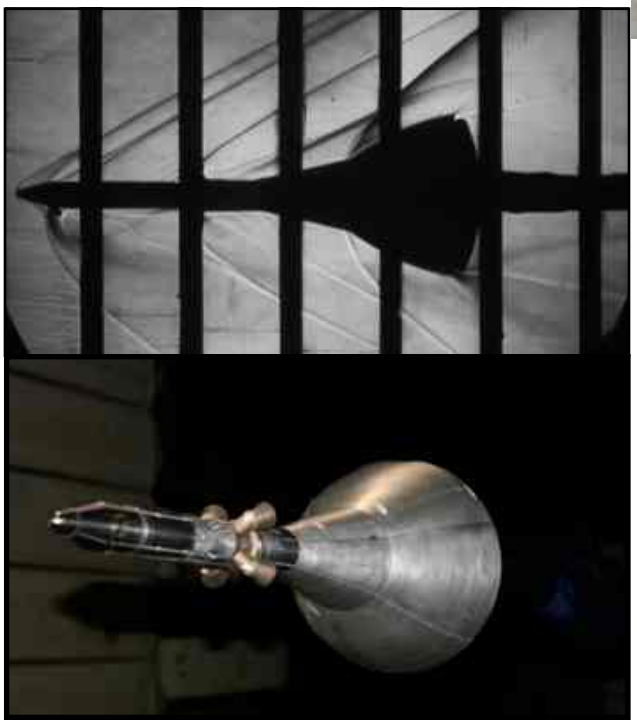

Figure 15. 5%-scale LAV model used for ACM jet interaction testing. Shadowgraph of a supersonic test in the NASA Langley Unitary Plan Wind Tunnel (top) and the 6%-scale model installation for transonic testing in the NASA Ames 11-Foot Transonic Wind Tunnel (bottom).

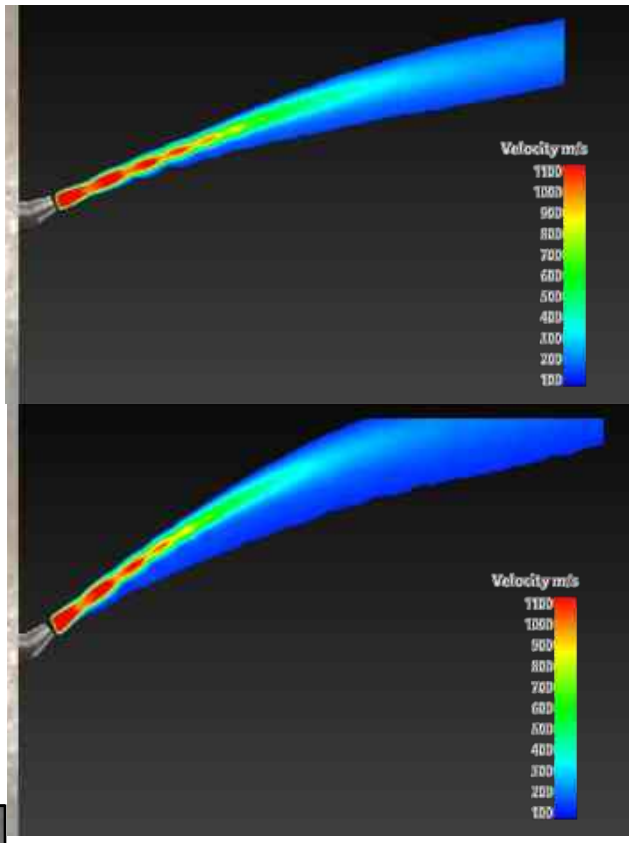

Figure 14. Velocity distribution measured in a plane bisecting the hot plume (~750K) measured using 3-component PIV. 25° nozzle (top) and 40° nozzle (bottom). No LAV model for these data.

3. ACM Jet Interaction Testing

Figure 15 shows two of the wind tunnel tests used to determine jet interactions for the ACM plumes.[25] For these tests flow through balances were either

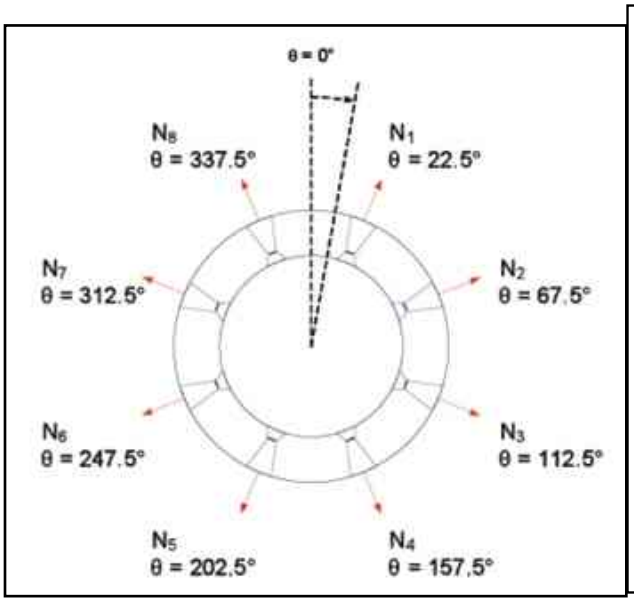

Figure 16. Cut through AMC nozzles just aft of LAV tower nose cone (see Figure 1).

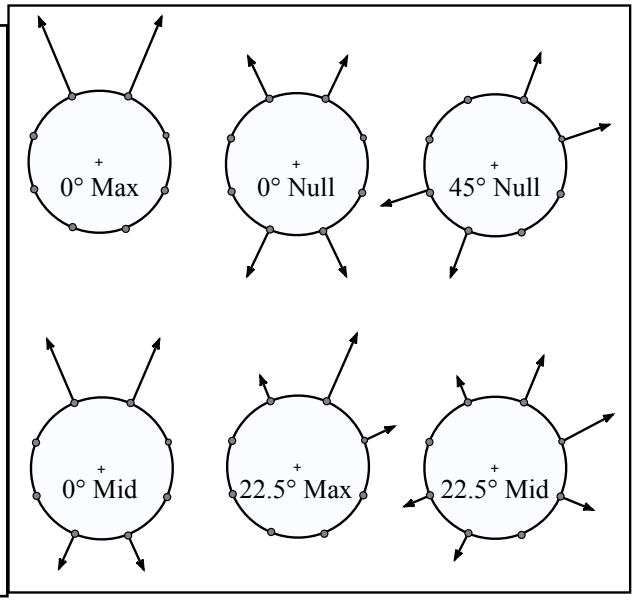

Figure 17. Examples of ACM firing direction and magnitude combinations.

available or were fabricated to match the pressure, mass flow, and load-range requirements. The only drawback to theses balances was the lack of axial measurement capability when the ACM flow path was pressurized. This proved to be only a minor drawback as the drag impact of the ACM plumes was a secondary test objective with the pitching moment being the primary objective of the tests.

A major complication to the ACM testing, however, is the way that the control motor works. The ACM is a solid rocket motor with eight throttle-able nozzles around the circumference of the Launch Abort Tower just below the nose cone (see Figure 1). There is essentially no limit to the combination of nozzle thrusts available to the control system except to maintain sufficient open area to limit the combustion-chamber pressure. Figure 16 shows the general arrangement of the ACM nozzles and the definitions developed to describe the ACM thrust magnitude and direction state. On the wind-tunnel model, individual nozzles could be mounted in each of the 8 nozzle locations to simulate a thrust direction and magnitude. The schematic in Figure 17 hints at how many potential combinations of nozzles and thrust levels can be provided by the ACM system. The fact that any number of nozzles from 2 to 8 can be active at a given time at a wide range of thrust levels means are nearly limitless combinations that might happen in the event of a launch abort. The control algorithm rules out some, but not many. Note that

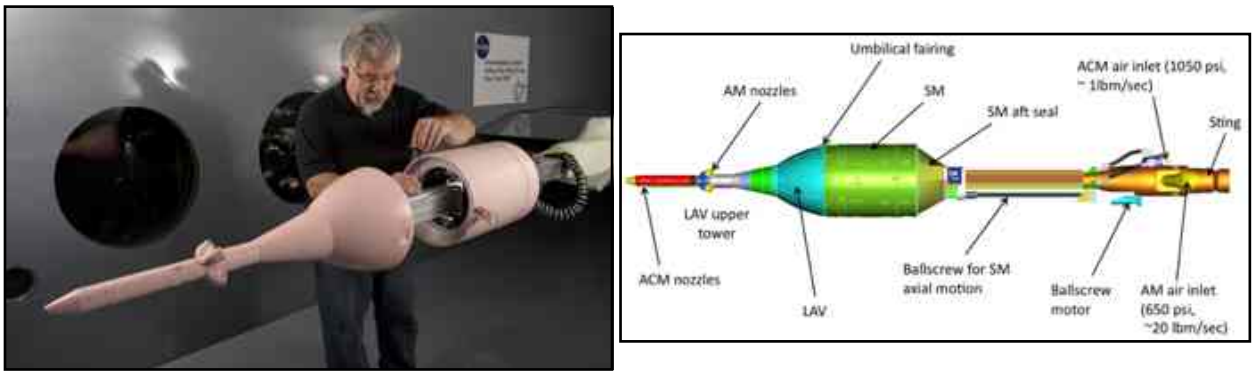

Figure 18. 6%-scale AM/ACM test model in the 9x7 Foot Wind Tunnel (left) and CAD rendering (right) that shows nozzle locations, high-pressure air supplies, and remotely positionable Service Module.

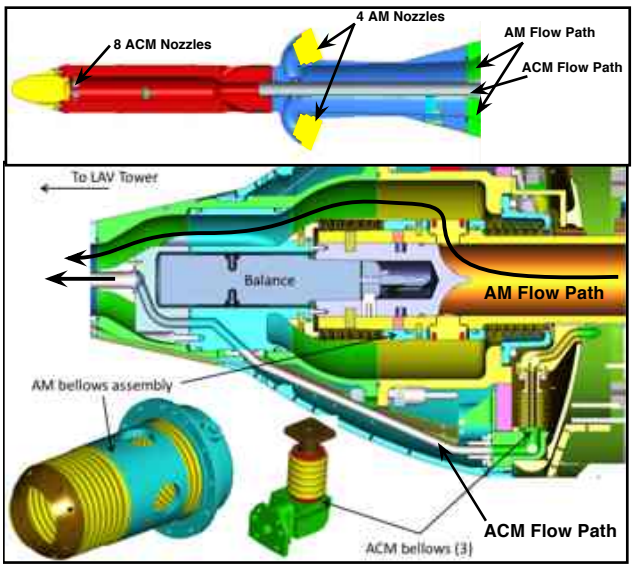

Figure 19. Section cut through LAV portion of the AM/ACM wind tunnel model. Bottom section shows the balance arrangement. Top sections shows air passages to AM and ACM nozzles.

even when commanding a zero net thrust (null cases in Figure 17) there is still a direction associated with it and the direction is not limited to 22.5° steps.

Because of time and cost limitations, a relatively small subset of potential ACM firing combinations were tested. During the two tests shown in Figure 15, more than 400 combinations of Mach number, dynamic pressure, and firing direction/magnitude were tested. In addition to this sparse coverage of wind-tunnel data, judiciously selected CFD cases were used along with response surfaces to stitch them together were used to generate the database.[26]

4.Combined ACM - AM Jet Interaction and Separation Aerodynamics Test

In order to provide sufficient separation distance between the crew and a failing launch vehicle, the Abort Motor generates thrust to accelerate the LAV at over 10 g's. That thrust comes with very large and energetic plumes that pass close to or envelope the LAV for the few seconds that the motor burns at full thrust. During that time the LAV control system must steer the vehicle away from the launch vehicle. With firm limits on the ACM thrust available and the unfavorable jet interactions that were measured and computed with CFD (both without the AM plumes) and measured in the ACM alone tests, control of the LAV can be marginal at some of the center of gravity locations expected in flight. Early AM jet interaction tests (without ACM simulations) provided some data on whether the large plumes helped or hurt the LAV stability - and of course the plumes did not help. The early tests had several deficiencies in the plume simulations and by leaving out the interaction with the ACM plumes, a test that included better AM plume simulations and simultaneous ACM simulations was needed. [27]

Designing a model to provide both AM and ACM plume simulations while accurately measuring the aerodynamic proved to be a challenge. There were no existing flow-through balances with 2 flow paths that could handle the pressure and mass flow required, the load range expected, and fit inside a model of a scale that could be tested up to Mach 2.5. That led to the model essentially being built around its own balance and bellows system.

Since we also needed to quantify the potential aerodynamic interference between the LAV and the launch vehicle as they separate during a launch abort, the model also included a model of the Service Module. The easy part of the model design turned out to be the remote actuation of the SM position relative to the LAV. The SM could be translated up to 1 diameter aft of the LAV and vertically ~0.25 diameter. It could also be pitched ±10° relative to the LAV. The model also included a remotely actuated umbilical fairing (Figure 18) that was programmed to open the appropriate amount for every separation distance and Mach number. The remote actuation was very effective in improving test productivity by eliminating all manual model changes for the SM.

Supplying the high-pressure air to both the AM and ACM nozzles proved to be the biggest challenge. Figure 19 shows a cutaway view of the model interior. Air for the two plume simulations pass through the model and around the balance using several high-pressure, edge-welded bellows. The two AM bellows form the inner surface of a plenum that surrounds the balance and the end of the sting. They also form a limber connection between the metric side of the balance and the non-metric sting. High-pressure air passes down the center of the sting and flows radially out through four large orifices into the plenum, around the balance, and then up the tower to the four AM nozzles.

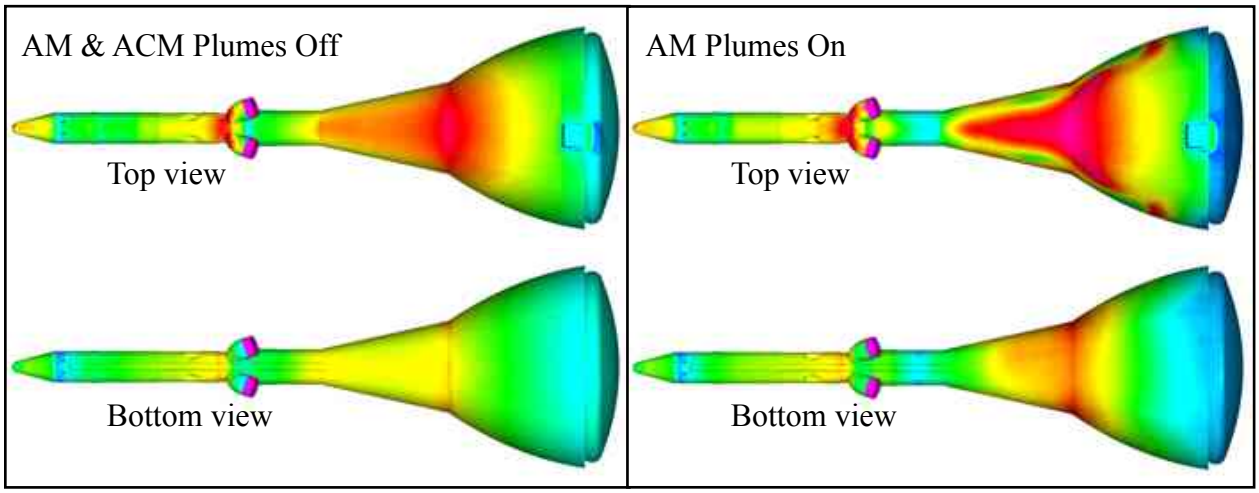

Figure 20. Example of PSP images from Orion powered LAV test. AM plumes off (left) and AM plumes on (right).[28]

The ACM flow path is along the outside of the sting in three stainless steel lines passing into the model through the heat shield immediately adjacent to the sting entry. An elbow fitting turns the flow radially which then passes through three bellows located 120° apart azimuthally. A second elbow in each of the 3 lines turns the flow back toward the tower and to the upper tower plenum and the eight ACM nozzles.

Development of the bellows required many iterations to meet the pressure and displacement requirements. There was also a requirement for sufficient fatigue life to survive at least the duration of an 8-week, double shift test. Each of the bellows designs were fatigue tested for both pressure cycling and motion cycling in excess of the expected cycles during the wind tunnel test. After the model was fully assembled, the balance and model were calibrated together for a large number of AM and ACM pressures. The accuracy was within the test requirements but was not as good as the measurement repeatability. That leaves the test team with a puzzle as to how to better interpret the calibration results so as to eliminate the remaining, unaccounted pressure tares - an effort that is continuing.

The test provided a large volume of data concerning the AM-ACM interactions as well as a more limited set of separation aerodynamics data. In spite of the long duration and high productivity, the very

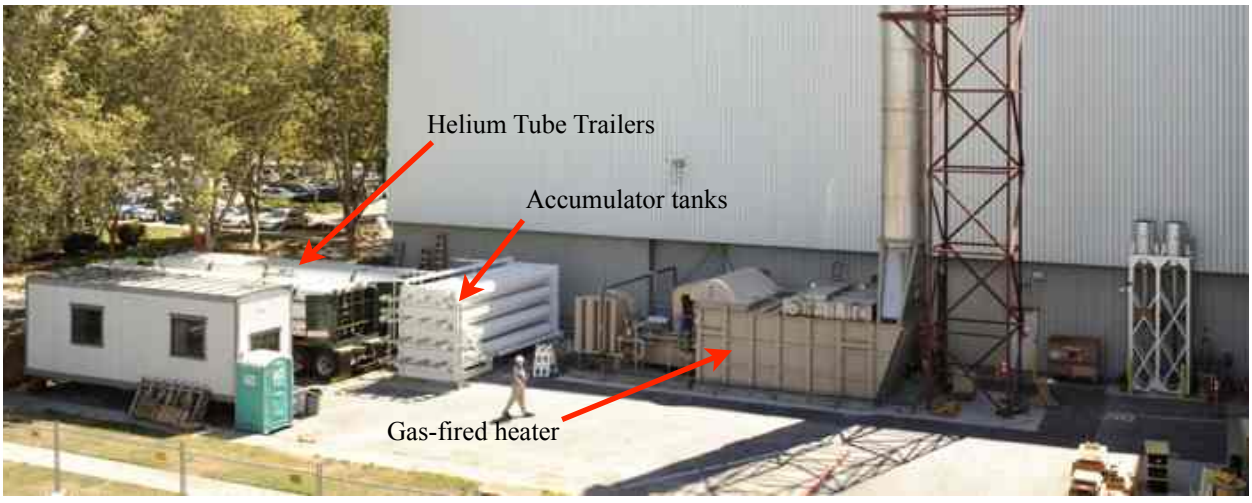

Figure 21. Helium supply system for Abort Motor plume aeroacoustics test in 11x11-Foot Transonic Wind Tunnel.

large number of ACM firing combinations and wide range of AM thrust ratios that could possibly happen during an abort meant that the aerodynamic database was constructed from a relatively sparse coverage of wind-tunnel data. This required the database team to perform careful fitting of response surfaces to the data and the data corrections in order to build an accurate database.[26]

Figure 22. Abort Motor plume acoustics test model in the wind tunnel.

A highlight of this particular test were the results of the PSP measurements. In the time between the PSP measurements made on the CM in 2006 and those made on the powered LAV model in 2010, the state of the art in PSP technology had improved tremendously. The advent of paints that self-correct for temperature has greatly improved the accuracy and repeatability of pressure measurement.[28] Figure 20 shows representative PSP images from the AM/ACM powered test. The PSP data was intended to be used primarily to develop the loads database but integrating the pressure over the surface of the model accurately reproduce the balance data, particularly for cases with no flow through the model's bellows. As the test results were examined, we discovered anomalies in the force and moment data caused by inaccurate pressure tares due to nonlinear behavior of the AM and ACM bellows. The PSP data allowed the test team to correct the balance for those conditions where there were unaccounted-for pressure effects further increasing the accuracy of the aerodynamic measurements.[26]

III. Abort Motor Plume Aeroacoustics Testing

As mentioned in above, the aeroacoustic loads on the LAV were an important input to the vehicle design. The nominal ascent loads were sufficiently large on the original design to warrant a radical

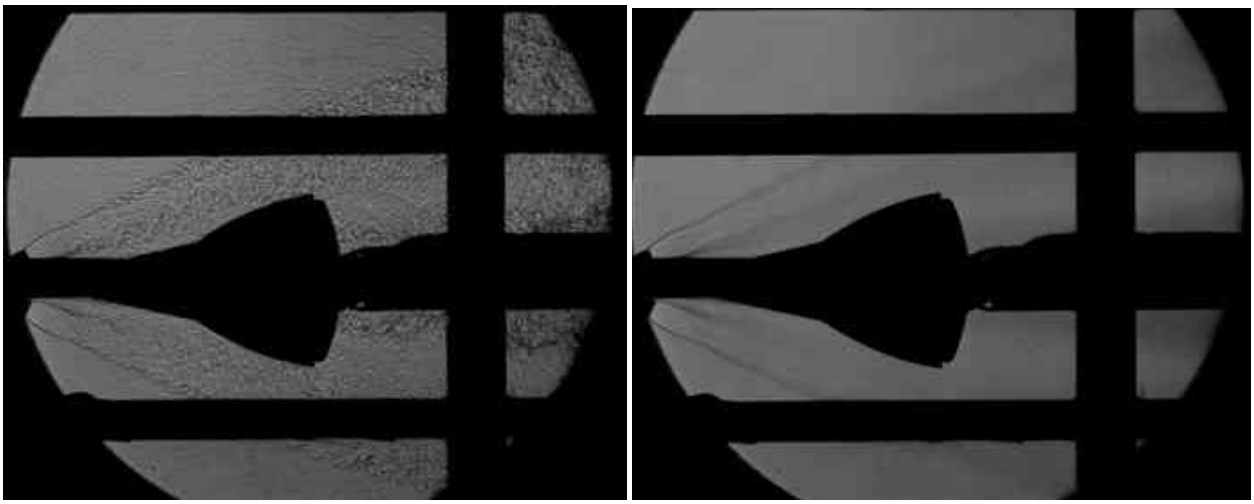

Figure 23. Shadowgraph images of hot Helium plume simulation for aeroacoustic loads test. Instantaneous image on left and average of 85 frames acquired at 5400 frames per second on right. Free-stream Mach number is approximately 0.5.

change in shape. During a launch or pad abort there is an additional aeroacoustic load on the LAV due to the AM plumes passing close to or enveloping the LAV surface so a series of lab experiments and wind-tunnel tests were conducted to provide accurate estimates of these loads. As with aerodynamic interactions, the hot plumes from a solid rocket motor generate very different acoustic signatures than a high-pressure air simulation of the plume in a wind tunnel. The primary reason for this is the strong dependence of the aeroacoustic on the plume velocity (more accurately, in the near field, this is fluctuating hydrodynamic pressure rather than acoustics). The speed of sound in a hot plume is more than twice that in the air simulations, so matching exit Mach number is no longer sufficient even with including the change is specific heat. The best simulation of the motor plume acoustics would employ a solid rocket motor but since the goal was to generate the aero-acoustic environment for all potential launch aborts (or at least the ones with the highest fluctuating pressure loads), the cost of such a wind tunnel test became prohibitive. A slightly less expensive path was chosen - simulating the plumes using heated Helium. This method of plume simulation allowed a much larger range of flight conditions to be simulated than would have been possible using a scaled solid motor. For a 6%-scale model, the plume simulation required that the Helium be supplied to the model at ~700 psi and ~700° F at a flow rate of up to 5 pounds-mass/second. A custom Helium supply system was developed for the test involving tube-trailers of He, a large bank of accumulator tanks, and a very high-capacity gas heater temporarily relocated from NASA Glenn Research Center. A photo of the supply system is shown in Figure 21. The helium consumption for the 2 weeks of testing was between 2 and 3 trailer loads per day. The model is shown in the test section in Figure 22. The orange tubes are the insulated supply lines for the helium. A total of 275 high-temperature unsteady pressure transducers were mounted in the model to record the fluctuation pressure levels. Each data point for the test consisted of a warm-up period with helium flowing with data being acquired only after the helium in model plenum reached the desired temperature and pressure. An automated control system provided stable and repeatable supply for the test.

Figure 23 shows two sample shadowgraph images from the test at a subsonic free-stream Mach number with the Helium plumes active. One of the images is a single image from a series of images acquired at 5400 frames per second. The other image is an average of all the images acquired at this condition. These images are compared to the expected plume structure to assess how well the plumes are modeled.[29]

IV. Summary

Wind-tunnel testing has played an important role in developing the aerodynamic database for atmospheric flight of the Orion spacecraft. Testing was also critical to properly shape the aerodynamic fairing used during launch and to define the aeroacoustic environment during nominal ascents and during any potential abort situations. Much of the testing involved relatively standard test techniques. Some tests, however, involved either extension of prior art or developing new hardware and mounting mechanisms for specific tests. For example, large amplitude forced oscillation testing was accomplished in the Transonic Dynamics Tunnel at NASA's Langley Research Center using a new oscillating model support system.

Powered testing posed an additional set of complications for a variety of reasons. Just adequately matching the characteristics of the available cold-air plumes to the expected hot plumes from the different solid rocket motors used during potential launch aborts proved difficult. The resulting plume simulations in the wind tunnel still need significant corrections developed using CFD in order to properly model the expected flight conditions. Simply performing the plume simulations with high-pressure air proved difficult because of the pressure levels and mass flows required. Simulation of a single motor was relatively straightforward, particularly for the low-thrust ACM tests since flow-through balances with the needed load range were available or could be readily built. Determining the interactions between the Abort Motor and Attitude Control Motor plumes and the Launch Abort Vehicle proved to be more difficult and required development of flexible high-pressure welded bellows and balance assembly to be the heart of the model resulting in extensive model calibrations. Even with those technique developments, the data still needed corrections based on integrated Pressure Sensitive Paint results to remove all of the pressure tares due to the bellows. All of these things came together at just the right time to provide accurate data to serve as the basis of the aerodynamic database.

V. Acknowledgements

The work summarized is represents many long hours put in by the members of the Orion Aerodynamics Testing team. Most of the tests required innovative solutions to a variety of challenges and only the creativity and perseverance of the various test teams led to the many successful tests. The engineers working on building the CFD parts of the aerodynamic database have also contributed to the success of the wind-tunnel tests and were active participants in most of the tests as have those tasked with building the database from its various sources.

References

[1] Ross, J. C., "Aerodynamic Testing in Support of Orion Spacecraft Development," AIAA 2007-1004, 45th AIAA Aerospace Sciences Meeting and Exhibit, Reno, NV, January 2007.

[2] Bell, J., "Transonic/Supersonic Wind Tunnel Testing of the NASA Crew Exploration Vehicle (CEV)," AIAA 2007-1006, 45th AIAA Aerospace Sciences Meeting and Exhibit, Reno, NV, January 2007.

[3] Murphy, K. J., "Testing of the Crew Exploration Vehicle in NASA Langley's Unitary Plan Wind Tunnel," AIAA 2007-1005, 45th AIAA Aerospace Sciences Meeting and Exhibit, Reno, NV, January 2007.

[4] Bell, J., "Comparison of Crew Exploration Vehicle (CEV) Tests in Two Supersonic Wind Tunnels," AIAA 2007-1008, 45th AIAA Aerospace Sciences Meeting and Exhibit, Reno, NV, January 2007.

[5] Murphy, K. J., Bibb, K. L., Brauckmann, G. J., Rhode, M. N., Owens, B., Bell, J. H., and Wilson, T. M., "Orion Crew Module Aerodynamic Testing," AIAA 2011-xxxx, submitted for presentation at the AIAA Applied Aerodynamics Conference, Honolulu, HI, June 2011.

[6] Bibb, K. L., "Development of the Orion Crew Module Static Aerodynamic Database, Part II: Subsonic," AIAA 2011-XXXX, AIAA Applied Aerodynamics Conference, Honolulu, HI, June 2011.

[7] Stremel, P. M., "Computational Aerodynamic Simulations of the Orion Command Module," AIAA 2011-XXXX, AIAA Applied Aerodynamics Conference, Honolulu, HI, June 2011.

[8] Bibb, K. L., "Development of the Orion Crew Module Static Aerodynamic Database, Part I: Hypersonic," AIAA 2011-XXXX, AIAA Applied Aerodynamics Conference, Honolulu, HI, June 2011.

[9] Bell, J. H., "Initial Characterization of Orion Crew Vehicle Aerodynamics Using Pressure Sensitive Paint," AIAA 2011-xxxx, submitted for presentation at the AIAA Applied Aerodynamics Conference, Honolulu, HI, June 2011. `

[10] Sellers, M. E., "AEDC's Portable Pressure-Sensitive Paint Data Acquisition System," AIAA 2007-1606, U.S. Air Force T&E Days, Destin, FL, February 2007.

[11] Chan, D. T., "Orion Flight Reynolds Number Testing in the NASA Langley National Transonic Facility," AIAA 2011-xxxx, submitted for presentation at the AIAA Applied Aerodynamics Conference, Honolulu, HI, June 2011.

[12] Moseley, W. C., and Hondros, J. G., "Aerodynamic Stability Characteristics of the Apollo Launch Escape Vehicle," NASA TN D-3964, June 1967.

[13] Tomek, D. M., Sewall, W. G., Mason, S. E., and Szchur, W. A., "Next Generation of High-Speed Dynamic Stability Wind Tunnel Testing," AIAA 2006-3148, 25th AIAA Aerodynamic Measurement Technology and Ground Testing Conference, San Francisco, CA, June 2006.

[14] Brown, J. D., Bogdanoff, D. W., Yates, L. A., and Chapman, G. T., "Static and Dynamic Aero Coefficients for Lifting CEV Capsules in Free Flight Between Mach 0.7 and Mach 1.25," AIAA Paper 2008-1232, 2008.

[15] Aubuchon, V.V., Owens, D.B., and Fremaux, C.M., "Drogue Parachute Effects on the Orion Capsule Aerodynamics," AIAA Paper 2011-????, presented at AIAA Applied Aerodynamics Conference, Honolulu, HI, June 2011.

[16] Owens, D. B., and Aubuchon, V. V., "Overview of Orion Crew Module and Launch Abort Vehicle Dynamic Stability," AIAA Paper 2011-????, 2011.

[17] Runckel, J. F., and Swihart, J. M., "A Hydrogen Peroxide Turbojet-Engine Simulator for Wind-Tunnel Powered-Model Investigations," NACA RM L-57H15, Washington DC, 1957.

[18] Berrier, B. and Pendergraft, O., Jr., "Transonic Aerodynamic Characteristics of a Powered Wind-Tunnel Model of the Apollo Launch-Escape Vehicle During Separation," NASA TM X-1336, Washington, D.C., April 1967.

[19] Childs, R. E., Garcia, J. A., Melton, J. A., Rogers, S. E., Setsopolov, A. J., Vicker, D. J., "Overflow Simulation Guidelines for Orion Launch Abort Vehicle Aerodynamic Analyses," AIAA 2011-XXXX, AIAA Applied Aerodynamics Conference, Honolulu, HI, June 2011.

[20] Rogers, S. E., "Computational Challenges in Simulating Powered Flight of the Orion Launch Abort Vehicle," AIAA 2011-XXXX, AIAA Applied Aerodynamics Conference, Honolulu, HI, June 2011.

[21] Brauckmann, G. J., Greathouse, J. S., and White, M. E., "Rocket Plume Scaling for Orion Wind-Tunnel Testing," AIAA 2011-XXXX, AIAA Applied Aerodynamics Conference, Honolulu, HI, June 2011.

[22] Rhode, M. N., Chan, D. T., Niskey, C. J., and Wilson, T. M., "Aerodynamic Testing of the Orion Launch Abort Tower Separation with Jettison Motor Jet Interactions," AIAA 2011-?, AIAA Applied Aerodynamics Conference, Honolulu, HI, June 2011.

[23] Wernet, M, Wolter, J. D., Locke, R., Wroblewski, A., Childs, R., and Nelson, A., "PIV Measurements of the CEV Hot Abort Motor Plume for CFD Validation," AIAA 2010-1031, 48th AIAA Aerospace Sciences Meeting and Exhibit, January 2010.

[24] Shestopalov, A. J., Childs, R. E., and Melton, J. E., "Turbulence Model Assessment for Hot Plumes," AIAA 2011-? Invited Paper presented at AIAA Applied Aerodynamics Conference Honolulu, HI, June 2011.

[25] Murphy, K. J., Brauckmann, G. J., Paschal, K. B., Chan, D. T., Walker, E. L., Foley, R. J., Mayfield, D. P., and Cross, J. N., "Orion Launch Abort Vehicle Attitude Control Motor Testing," AIAA 2011-XXXX, AIAA Applied Aerodynamics Conference, Honolulu, HI, June 2011.

[26] Chan, J., "Modeling Powered Aerodynamics for the Orion Launch Abort Vehicle," AIAA-2011-?, submitted for presentation at the AIAA Applied Aerodynamics Conference, Honolulu, HI, June 2011.

[27] James, K. D., "Title," AIAA-2011-?, submitted for presentation at the AIAA Applied Aerodynamics Conference, Honolulu, HI, June 2011.

[28] Sellers, M. E., "Demonstration of a Temperature-Compensated Pressure Sensitive Paint on the Orion Launch Abort Vehicle," AIAA 2011-?, submitted for presentation at the AIAA Applied Aerodynamics Conference, Honolulu, HI, June 2011.

[29] Panda, J., James, G. H., Burnside, N. J., Fong, R. K., Fogt, V. A., and Ross, J. C., "Use of Heated Helium to Simulate Surface Pressure Fluctuations on the Orion Launch Abort Vehicle During Abort Motor Firing," AIAA 2011-XXXX, AIAA Aeroacoustics Conference, Portland, OR, June 2011.

Appendix A -

Table 1. List of Orion Wind Tunnel Tests to date sorted by type of test.

Test Number	Type	Date	Facility	Description
50-AS	**Ascent acoustics**	5/17/07	Boeing Polysonic Wind Tunnel (PSWT)	A preliminary investigation into the aeroacoustic loads generated by the Pad Abort Test (PA-1) LAV configuration and the potential reduction in those loads provided by an alternate Launch Abort System configuration (ALAS-2 mod-1) developed by the ALAS project of the NESC.
58-AA	**Ascent acoustics**	10/8/07	Arnold Engineering and Development Center (AEDC) 4T	Test to identify LAV configuration to adopt for flight. Down-select between ALAS-11 rev 3, rev 8, and rev 10. Approximately 12 flush mounted microphones
57-AS	**Ascent acoustics**	11/1/07	NASA Glenn Research Center (GRC) 8x6	LAV Ascent Aeroacoustics comparing PA-1 and ALAS-11 rev. 3 configurations with approximately 100 surface mounted microphones
11-CD	**Dynamic stability**	4/8/06	US Army Aberdeen Test Range	Proof of concept test to evaluate the Aberdeen Research Laboratory telemetry technique for ballistic range test data acquisition and analysis of CM flight.

Test Number	Type	Date	Facility	Description
8-CD	**Dynamic stability**	5/10/06	NASA Langley Research Center (LaRC) Transonic Dynamics Tunnel (TDT)	Small-amplitude forced oscillation test of CM w/ some unsteady pressures.
12-CD	**Dynamic stability**	6/19/06	US Army Aberdeen Test Range	Evaluation of improved sabot designs for CM testing at the Aberdeen Test Range
13-CD	**Dynamic stability**	7/6/06	US Air Force Eglin Ballistic Range	Transonic and supersonic dynamic aero data for zero L/D CM model
15-CD	**Dynamic stability**	9/2/06	US Army Aberdeen Test Range	Lifting and non-lifting CM models for dynamic aero database development
14-CD	**Dynamic stability**	10/5/06	NASA Ames Research Center Hypersonic (ARC) Free-Flight Aerodynamics Facility	Transonic and supersonic dynamic aero data of CM at non-zero L/D
18-CD	**Dynamic stability**	1/1/07	LaRC TDT	Demonstration of Oscillating Turn Table test technique in the TDT to obtain dynamic stability of the CM at high Reynolds numbers. Comparisons with ballistic range data and previous small-amplitude forced oscillation test (8-CD)
48-CD	**Dynamic stability**	3/1/07	LaRC Vertical Spin Tunnel (VST)	Free-flight test of CM at low Mach number to provide dynamic stability estimates for the Pad Abort flight test.
52-CD	**Dynamic stability**	3/1/07	ARC Fluid Mechanics Laboratory Test Cell 2 (TC-2)	Test technique development to examine issues related to Free-to-Oscillate testing. Will duplicate the conditions of 48-CD test of the CM.
45-AD	**Dynamic stability**	3/9/07	LaRC VST	Low-Mach number test of LAV in support of PA-1 Flight Test
29-CD	**Dynamic stability**	6/1/07	ARC Gun Development Facility	Phase 2 of CM dynamic stability at large angles of attack.
82-AD	**Dynamic stability**	12/21/0	LaRC VST	Forced Oscillation test of LAV in the Vertical Spin Tunnel
27-AD	**Dynamic stability**	3/21/08	LaRC TDT	Forced oscillation (subsonic and transonic) test of LAV and CM through as much of the 0-180 deg. range as possible.
108-CD	**Dynamic stability**	8/25/09	Bihrle Research VST	Low-speed dynamic stability test to support Orion decisions on back shell angle changes.

Test Number	Type	Date	Facility	Description
109-CD	**Dynamic stability**	11/15/0	LaRC VST	Dynamic stability of CM under parachutes.
117-CD	**Dynamic stability**	4/1/10	LaRC VST	Phase 2 of dynamic stability test of CM under parachute
46-AD	**Dynamic stability**	6/1/10	US Air Force Eglin Ballistic Range	Ballistic range test of LAV.
55-AS	**Plume Acoustics**	9/28/07	Florida State Jet Noise Laboratory	Series of hot- versus cold-jet acoustic experiments to possibility develop scaling laws to allow the use of cold plume tests for the LAV with AM firing. Phase 1 - 2" 2,000°F jet versus 2" cold jet. Phase 2 - Same 2 jets with more measurement locations. Phase 3 - ~1" D nozzle exit hybrid rocket. Phase 4 - Sounding rocket motor plume noise measurements at NASA Wallops Flight Facility.
51-AS	**Plume Acoustics**	10/30/0	ARC Unitary Plan Wind Tunnel (UPWT)	6%-scale LAV model test to determine the aeroacoustic loading generated by cold air simulation of the AM plumes. ~200 flush microphones.
80-AS	**Plume Acoustics**	9/20/10	ARC UPWT	Hot Helium simulation of AM plumes for acoustic loads. ~200 flush microphones.
53-AA	**Plume Jet Interaction (JI)**	5/21/07	Texas A&M 7x10 Foot Wind Tunnel	First test of subsonic interactions between the ACM plumes and the LAV. Primarily to validate CFD and to provide some data on coast-phase ACM increments for the PA-1 flight test aero database.
16-AA	**Plume JI**	6/22/07	ARC UPWT	Abort loads on the CM due to AM plume JI and proximity to Service Module
59-AA	**Plume JI**	9/14/07	ARC UPWT	High fidelity ACM JI for both Pad Abort-1 flight test article and production ALAS-11rev3B configuration.
60-AA	**Plume JI**	1/30/08	ARC UPWT	Preliminary separation aerodynamics during abort initiation on PA-1 and ALAS-11 rev3B configurations. Preliminary aeroacoustics for nominal ascent (with SM) and abort (LAV only) with cold air plume simulation.
85-AA	**Plume JI**	8/20/08	GRC Aero-Acoustic Propulsion Laboratory	CFD validation test documenting flowfield associated with single AM nozzle at M < 0.3 using PIV. Nozzle at 0°, 25°, and 40° relative to free stream. With and without simplified LAV model.
61-AA	**Plume JI**	12/1/08	LaRC 14- by 22-Foot Wind Tunnel	Subsonic 6%-scale Jettison Motor Jet Interaction test around alpha = 180°.
24-AA	**Plume JI**	6/25/09	AEDC 16T	Transonic/supersonic test of Jettison Motor Jet Interation for LAS jettison during a launch abort (i.e. heat shield forward).
75-AA	**Plume JI**	7/24/09	ARC UPWT	Subsonic, transonic, and low-supersonic ACM Jet Interaction test.

Test Number	Type	Date	Facility	Description
76-AA	**Plume JI**	11/24/0	LaRC UPWT	Supersonic ACM Jet Interaction test (M 1.6 to 4.6).
25-AA	**Plume JI**	2/26/10	ARC UPWT	Supersonic (M 1.6 to 2.5) Jettison Motor Jet Interaction and Jettison LAS/CM Proximity aerodynamics.
26-AA	**Plume JI**	8/9/10	ARC UPWT	Subsonic, transonic, and supersonic AM and ACM Jet Interactions including separation effects data for the LAV. PSP to document pressure loadings during launch aborts.
3-CA	**CM Static Aero**	2/10/06	LaRC UPWT	Study of BL trip techniques on 3%-scale CM model.
7-CA	**CM Static Aero**	3/10/06	LaRC UPWT	Force and moment measurements & pressure distributions, with apex cover on/off and boundary-layer transition/tripping study.
5-CA	**CM Static Aero**	3/22/06	ARC UPWT	Force & moments and pressure data on 7.5%- and 3%-scale models. Provided tunnel-to-tunnel comparisons between LaRC and ARC UPWT.
9-CA	**CM Static Aero**	4/20/06	LaRC Mach 6 Tunnel	3%-scale CM test for alpha from 0 to 180°.
1-CA	**CM Static Aero**	12/8/06	LaRC UPWT	Boundary layer transition measurements with IR thermography and Temperature Sensitive Paint.
19-AA	**LAV Static Aero**	1/29/07	Boeing PSWT	3%-scale transonic test of PA-1 LAV configuration for 0-180° angle of attack.
54-AA	**LAV Static Aero**	4/13/07	Lockheed High-Speed Wind Tunnel	Quantify the roll coupling with angle of attack caused by the clocking of the abort motor nozzles on the PA-1 configuration. Study effectiveness of various nozzle fairings in relieving the roll interaction.
88-AA	**LAV Static Aero**	10/20/0	LaRC VST	Test of the PA-1 Launch Abort Tower alone to define the post-jettison aerodynamics.
83-AA	**LAV Static Aero**	6/1/08	LaRC National Transonic Facility	High-Re effects on unpowered LAV aerodynamics.
122-PA	**Static Aero**	11/8/10	ARC TC-2	Small-scale test of Forward Bay Cover aerodynamics to validate CFD and engineering models of the FBC jettison event.